NANO LETTERS

Letter

pubs.acs.org/NanoLett

Dynamic Control of the Vortex Pinning Potential in a Superconductor Using Current Injection through Nanoscale Patterns

Yoav Kalcheim,*[,†,§] Eran Katzir,[‡] Felix Zeides,[†] Nadav Katz,[†] Yossi Paltiel,[‡] and Oded Millo[†]

[†]Racah Institute of Physics and the Center for Nanoscience and Nanothechnology and [‡]Applied Physics Department and the Center for Nanoscience and Nanothechnology, The Hebrew University of Jerusalem, Jerusalem 91904, Israel

Supporting Information

ABSTRACT: Control over the vortex potential at the nanoscale in a superconductor is a subject of great interest for both fundamental and technological reasons. Many methods for achieving artificial pinning centers have been demonstrated, for example, with magnetic nanostructures or engineered imperfections, yielding many intriguing effects. However, these pinning mechanisms do not offer dynamic control over the strength of the patterned vortex potential because they involve static nanostructures created in or near the superconductor. Dynamic control has been achieved with scanning probe methods on the single vortex level but these are difficult so scale up. Here, we show that by applying controllable nanopatterned current injection, the superconductor can be locally driven out of equilibrium, creating an artificial vortex potential that can be tuned by the magnitude of the injected current, yielding a unique vortex channeling effect.

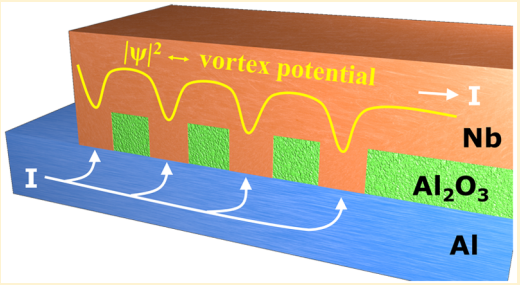

KEYWORDS: *Superconducting vortices, vortex manipulation, artificial vortex pinning, nonequilibrium quasiparticle distribution, superconductivity*

Pinning of vortices accounts for many of the electrical and magnetic properties of type II superconductors (S). As such, this field has been intensively studied for many decades both in conventional[1] and high T_c superconductors.[2] Intrinsic pinning due to material imperfections along with intervortex interaction results in a very rich phase diagram for vortex matter.[3−7] In the past two decades, extensive efforts have been dedicated to creating artificial pinning potentials that can be controlled spatially. One way to achieve this is by placing magnetic nanoparticles in the vicinity of an S film[8,9] or embedding them in a wire.[10] The interaction of the vortex field with the magnetic particles lowers the energy for the vortex to reside near them, thus creating a pinning potential. Alternatively, one can create potential wells for vortices using artificial defects, which locally reduce the condensation energy. Numerous methods have been implemented to produce condensation energy landscapes, including thickness modulations, proximity to normal metal dots, ion irradiation damage, multilayers, and wire networks of superconductors.[11−20] Some also take advantage of the intrinsic anisotropy in high-T_c superconductors to control vortex motion using fine-tuned alternating (ac) currents and magnetic fields.[21] Studies of artificial pinning based on these mechanisms have shown fascinating phenomena. These include locking of the vortex lattice onto the ordered artificial pinning array manifested as sharp features in magneto-resistance[22] and magnetization curves,[10] and voltage rectification due to vortex ratchet effects.[23−27] Work on vortex dynamics in curved superconductors has also shown control over vortex nucleation using inhomogeneous transport current.[28,29] Most recently, control over the motion of individual vortices has been shown by applying local stress using a sharp tip,[30] focused light,[31] and an STM tip[32] and manipulation of Josephson vortices has been suggested using edge currents in adjacent superconducting electrodes.[33]

However, all scalable artificial patterned pinning mechanisms studied so far suffer from a common shortcoming; once the pinning potential has been created it is no longer possible to control its magnitude or its spatiotemporal evolution. In this Letter, we show that such dynamic control can be achieved by using localized current injection to create a vortex potential landscape corresponding to the (predesigned) current injection nanopattern. By changing the intensity of the injected current, the magnitude of the potential can be varied over time. This paves the way toward precise dynamical vortex manipulation. We explore three patterns of current injection whereby we induce channeling of vortex flow and also succeed in directing vortices in a trajectory that deviates from that of the force exerted on them by the current.

The creation of a vortex potential landscape by current injection relies on the suppression of the order parameter in the S due to nonequilibrium quasiparticle (QP) occupation. It is well established that deviations of QP distributions from the Fermi−Dirac distribution can cause enhancement or reduction

Received: January 13, 2017
Revised: April 11, 2017
Published: April 13, 2017

DOI: 10.1021/acs.nanolett.7b00179
Nano Lett. 2017, 17, 2934−2939

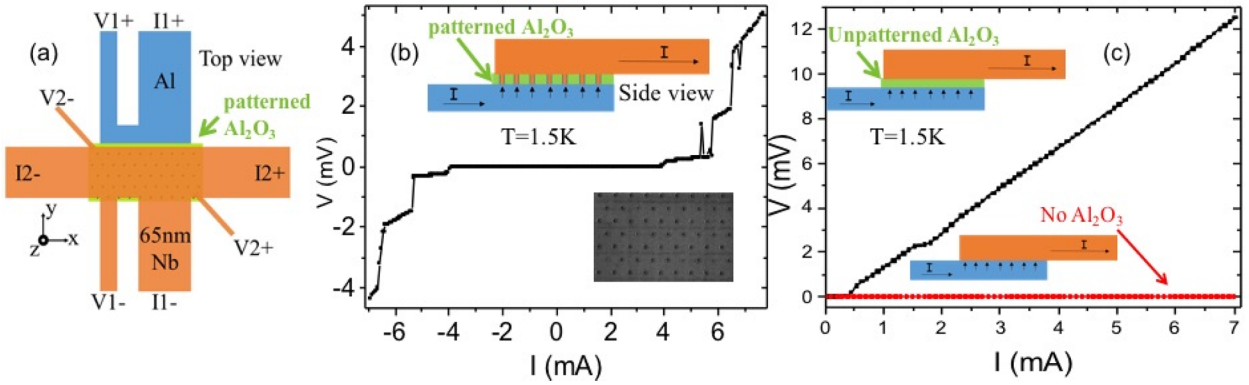

Figure 1. (a) Sample configuration (see also text): Current leads are $I1\pm$ ($I2\pm$) and voltage is measured between $V1\pm$ ($V2\pm$), correspondingly. (b) $V1\pm$ versus $I1\pm$ measurements at 1.5 K of Nb/Al_2O_3/Al samples where the intermediate Al_2O_3 is patterned with a triangular array of holes, as shown in the SEM micrograph of the Al_2O_3 pattern before deposition of the Nb layer (see inset: lattice constant is 600 nm). Voltage jumps indicate opening of vortex channels across the sample. (c) Same measurement as in (b) but on samples without a pattern; either Nb/unpatterned-Al_2O_3/Al (black curve) or Nb directly on Al (red). No voltage jumps are observed in both cases.

of the gap relative to its equilibrium value, depending on the type of deviation.[34,35] This originates from the self-consistent BCS gap equation which relates the QP occupancy f_k to the gap magnitude Δ

$$\frac{2}{V} = \sum_k \frac{1 - 2f_k}{(\Delta^2 + \xi_k^2)} \quad (1)$$

where V is the electron−electron coupling strength and ξ_k is the energy with respect to the Fermi level; this equation remains approximately valid even for an out-of-equilibrium QP occupancy.[34] Strikingly, Blamire et al. demonstrated a two-fold enhancement of the critical temperature of a superconductor when QPs are extracted from it, thus creating a QP distribution corresponding to lower temperatures.[36] This requires tunnel junctions involving superconductors with different gap magnitudes. The opposite effect, where the gap is suppressed with QP injection, is more common and occurs when current flows from a normal metal into the superconductor. Charge enters the S either as QPs with energy larger than the gap or as evanescent waves for subgap states, which decay into the condensate with a characteristic decay length of ξ_S, the superconducting coherence length.[37] The order parameter will thus be suppressed near the region of current injection and recover over a length scale of the QP diffusion length, typically larger than ξ_S.[38,39] In an S film subjected to high QP injection, not only will the gap be suppressed but one also finds instability toward a state of multiple reduced gaps in different regions in S. This is because above a threshold injection current, the gap in a certain region may be sufficiently suppressed, so that more QPs from its vicinity are attracted there, leading to spatially inhomogeneous QP populations and gap magnitudes.[40−42] Our present work shows that by injecting current into S films in a local manner, the effect of nonequilibrium QP distribution and gap reduction can be harnessed to produce a vortex potential landscape, which enables control over vortex motion.

Samples were prepared using standard e-beam and photolithography techniques as described in the Supporting Information. The samples consisted of Al and Nb films separated by 20 nm thick Al_2O_3 containing various patterns of holes through which direct contact between the Nb and Al was achieved. The measurements were conducted at temperatures between the Al and Nb superconducting critical temperatures, so that the Al film can be regarded as a normal metal. Current leads were connected either to the Nb only or to the Nb and the Al, with corresponding voltage leads, making it possible to isolate the effect of current passing through the patterned holes in the Al_2O_3 layer from possible effects on the Nb film resulting from their mere presence.

Figure 1a shows a scheme of the sample with the two main measurement configurations which were employed. In the first, the current and voltage contacts used were $I1\pm$ and $V1\pm$, respectively. Evidently, in this configuration current must flow through the patterned Al_2O_3. In the second configuration, the current flows through contacts $I2\pm$, which are both on the Nb layer, and voltage is measured through $V2\pm$. Here, below the superconducting transition of Nb current will only flow through the Nb, thus providing a control for the first configuration using the very same sample, as will be discussed in the following. Except for Figure S1 in the Supporting Information, all measurements presented here were performed using the first configuration ($I1\pm$ and $V1\pm$).

Figure 1b shows a $V(I)$ curve acquired at 1.5 K for a sample with an Al_2O_3 pattern consisting of a triangular array of 200 nm diameter holes with lattice constant of 600 nm (see inset). For low currents, the voltage is zero to the measurement resolution, indicating high enough interface transparency for injection of subgap QPs. As the current increases the voltage rises abruptly in a series of jumps. Between the jumps, the voltage progresses linearly with a slope that increases after each jump. The width of the jumps increases with temperature (not shown). In contrast, no voltage jumps are observed in a similar sample that consists of an unpatterned Al_2O_3 layer between the Nb and Al (Figure 1c). Instead, a much smaller critical current is observed and the voltage progresses smoothly without any jumps. We attribute the zero voltage portion of the $V(I)$ to unintentional pinholes in the Al_2O_3 layer. In the absence of an Al_2O_3 layer, no voltage is detected up to currents as high as 30 mA. The pattern thus plays an important role in inducing the observed voltage jumps. This effect is qualitatively insensitive to the exact array configuration (hole size, spacing, and array shape). If, however, a patterned sample is measured in the second configuration (current, $I2\pm$, and voltage, $V2\pm$, in Figure 1a), where current contacts are made only to the Nb, no observable voltage is found for currents as high as 30 mA. To achieve comparable voltage magnitudes as in the first configuration the sample had to be heated very close to the Nb critical temperature (T_c =

DOI: 10.1021/acs.nanolett.7b00179
Nano Lett. 2017, 17, 2934−2939

8.36 K) but then the voltage rose smoothly with current and no jumps were observed (see Figure S1). Thus, it is clear that the mere presence of the holes' pattern over which the Nb film is grown does not suffice for observation of voltage jumps. The current must pass through the pattern in order for the jumps to occur. We can thus exclude any static pinning potential effects arising from the patterned Al_2O_3 underlying the Nb as the origin of the voltage jumps.

The jumps also have an intricate dependence on the magnetic field, which was applied perpendicular to the sample plane. Namely, all voltage jumps occur at currents that decrease with increasing field, as shown in Figure 2. Because the field

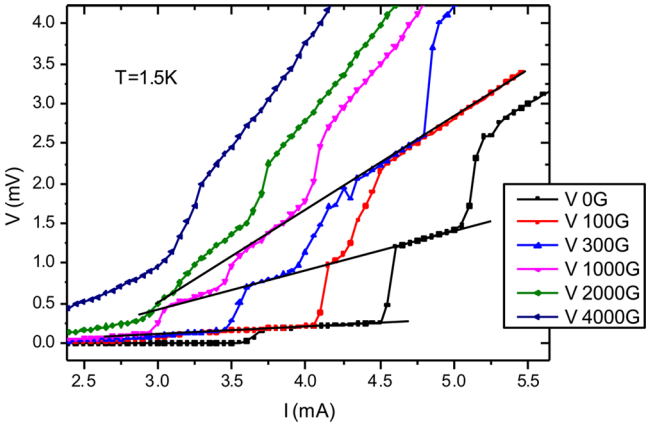

Figure 2. V versus I measurements under applied out-of plane magnetic field at T = 1.5 K. Solid lines are a guide to the eye. For fields up to 1000 G, straight lines connect linear segments of the different curves. In this range, vortex flow is mainly restricted to channels. The magnetic field only has the effect of opening the channels at lower currents but negligibly affects the conduction within each channel. This is no longer true at higher fields.

increases vortex density, this strongly indicates that the onset of vortex flow is at the origin of the observed voltage jumps. It is important to recall that even without an external field, the field produced by the current itself is on the order of 100 G per milliamp at the edge of the sample for this geometry. Consequently, considerable vortex density is present when voltage jumps appear even in the absence of an applied field. For instance, the self-field at the edge of the sample for the first jump in Figure 1 at 4 mA corresponds to a mean intervortex distance of 240 nm.

It is unlikely to account for this phenomenology by assuming homogeneous vortex flow because this would mean that the mobility of all vortices increases sharply in several jumps. Instead, it is more natural to assume that vortex flow is inhomogeneous in the sample, where vortices flow across the sample in the form of channels or filaments from one side of the junction to the other. If the force exerted by the current exceeds the pinning force at a particular location, vortex flow will nucleate there while in other regions vortices remain static. Every voltage jump is then interpreted as the opening of another vortex channel due to the surpassing of a local critical current. Indeed, theoretical and experimental work from the last two decades have established that voltage jumps followed by linear progression of the voltage with current are a manifestation of vortex channeling in type II conventional and high T_c superconductors.[43−47] However, to the best of our knowledge this work constitutes the first observation of channeling controlled by patterned current injection. Note also that for fields up to 1000 G straight lines with the same slope and intercept fit the linear segments (between jumps) of the $V(I)$ curves acquired at different magnetic fields. This suggests that for fields close to the self-fields induced by the applied current, vortex flow is restricted to the same channels that open more easily with increasing field, whereas, once the channel is open, the flow magnitude is determined primarily by the current, consistent with molecular dynamics simulations of plastic flow (see ref 46 for more details on the $V(I)$ characteristics of filamentary vortex flow).

One might suggest that the observed voltage jumps occur because the critical current is locally attained due to the confinement of the current to the holes in the pattern. However, even if one assumes that the entire current flows through the Nb film to its edge and is then transmitted to the Al through the last row of holes, the combined cross-sectional area through which the current is confined will be only 0.8 of the cross section of the film itself. From the measurement of the critical current in the same film with the current applied in the perpendicular direction through the Nb only (using leads labeled 2 in Figure 1), we find that at least 40 mA would be required to flow through that row of holes to reach the critical current of the Nb film. However, as shown in Figure 1, the first jump is observed already at 4 mA, an order of magnitude lower, thereby ruling out simple confinement of current as the cause for channeled vortex flow. We are thus led to the conclusion that the pinning force acting on the vortices is decreased by at least 10 times with respect to its intrinsic value. We note that for the Nb to turn normal due to depairing, much larger currents are required and thus vortex depinning would precede total suppression of the order parameter. Even if one assumes that in our case all the current flows through only one row of holes, the typical depairing current density in thin and nanostructured Nb films would be around $3-6 \times 10^7$ A/cm^2,[48−50] corresponding to a current of ∼1 A for our geometry. This value is at least 2 orders of magnitude larger than the currents we applied.

We suggest that the origin for the observed vortex channeling effect is that confined injection of current through the holes in the Al_2O_3 creates inhomogeneous QP populations that locally reduce the pinning force on vortices, resulting in a vortex potential that favors flow in the form of channels. According to the Larkin−Ovchinnikov model for vortex flow,[51] once vortex motion begins the resulting electric field accelerates QPs trapped in the vortex cores so that they may gain enough energy to be released from the core. In turn, this enhances vortex mobility leading to an avalanche-like effect. In our case, it is possible that the confinement of QPs limits this effect spatially, thus creating the multiple channel behavior for each region individually. Another possible consequence of QP injection through holes is that as the current is increased, the QP-rich regions around the holes grow to the point that they start to overlap, thus enabling vortices to move more easily between them in a percolative manner that also favors channel formation. As discussed in ref 40, for low current injection QPs will diffuse away from the current injection region, whereas after a certain threshold magnitude the gap is sufficiently suppressed locally for the injected region to attract more QPs leading to a runaway effect. This can explain why voltage jumps appear in patterned samples but not in the sample with no Al_2O_3 layer, because in the latter the area of direct contact

DOI: 10.1021/acs.nanolett.7b00179
Nano Lett. 2017, 17, 2934−2939

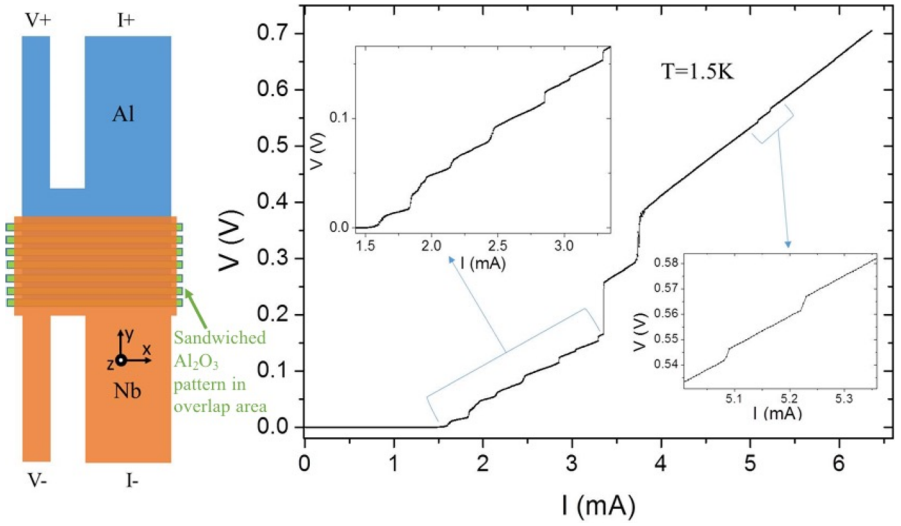

Figure 3. V versus I of a multiple horizontal channel sample as shown in the measurement scheme. The actual sample consisted of 15 horizontal lines of Al_2O_3 between the Al and Nb layers. The line separation and width is 2 μm. The number of voltage jumps (13) is close to the number of lithographically defined channels (see text).

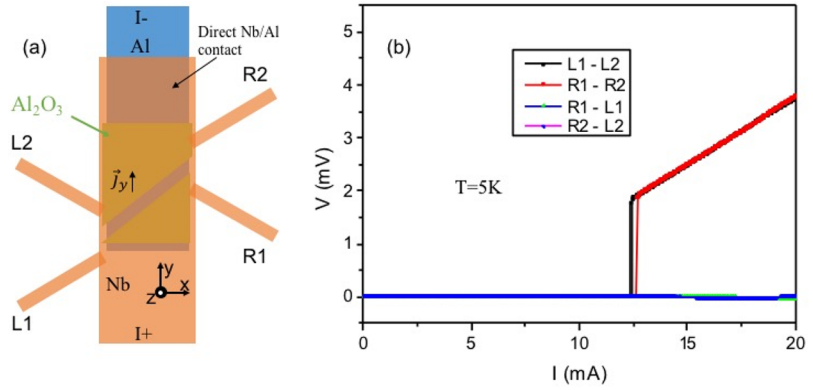

Figure 4. V versus I curves measured at T = 5 K on a sample with a single channel fabricated at an angle with voltage leads at the channel edges, as shown in the scheme (a). Most of the current flows from the Nb to the Al through the top section where the Al_2O_3 layer is absent. The channel serves to modulate the pinning potential. Voltage is measured using the four electrodes protruding from the structure, while current is applied along the y-direction. (b) V versus I measured using different voltage leads, as indicated. A single voltage jump, consistent with a single vortex channel, appears only when voltage is measured across the channel. No jumps are observed for electrodes on the same side of the channel.

between the Al and Nb is 8 times larger so that the QP instability threshold current density may not be locally attained.

To clarify the mechanism at the origin of the channeling effect and achieve more control over it, we fabricated samples in which the Al_2O_3 pattern was in the form of straight parallel lines running along the x-direction, as in a crossroad, where the current flows perpendicularly in the y-direction (see Figure 3). The area of direct contact between the Al and Nb in this pattern is half of their total overlap area, thus making the current density similar to that of an unpatterned sample with no inhomogeneity in the x-direction. Thus, the force exerted on vortices by the current should be very similar to that of a sample without the Al_2O_3 layer. However, the QP distribution would still follow the pattern and show a modulation in the form of continuous lines along the x-direction, parallel to the force exerted on the vortices. Thus, channeling of vortices is expected to be more efficient in this sample. Indeed, as shown in Figure 3, the $V(I)$ curve of such a "crossroad sample" shows 4 times more jumps compared to the hole array sample for the same current range. Moreover, the typical jump size is 2−3 times larger than the jumps observed in the hole array, indicating higher vortex mobility. However, because the two samples were not fabricated together in the same run, this comparison may not be a valid one due to differences in normal state resistivities and the Nb/Al interfacial properties.

A clearer indication for the effect of this pattern on the channeling effect is provided by the good correlation between the number of voltage jumps and the number of channels in the pattern. In Figure 3, 13 voltage jumps are observed whereas the number of lithographically defined channels in the pattern was 15. However, close inspection of the large voltage jump at 3.69 mA reveals that it actually consists of two jumps taking place simultaneously. This is most easily observed by taking a time trace of the voltage at the current for which the jump occurs (3.69 mA), which reveals three metastable states (Figure S2). This might be a consequence of the influence of one channel on the other, where QPs leak between adjacent channels so that they merge, trigger the opening of additional channels, or synchronize their order parameter oscillations.[52] For more details on the interaction between phase slip centers see refs 53 and 54. The voltage jump at 3.4 mA, which is significantly larger than other typical jumps, may also be a result of the

DOI: 10.1021/acs.nanolett.7b00179
Nano Lett. 2017, 17, 2934−2939

opening two channels together (albeit without multistability as in the jump at 3.69 mA) thus bringing the total number of voltage jumps to 15 corresponding to the 15 lithographically defined channels. Even more direct evidence for the link between a lithographically defined channel and a single voltage jump is provided by the following experiment.

We now turn to address the question of whether localized current injection simply facilitates vortex flow in its vicinity or whether it actually creates a potential that can exert a nontrivial force on vortices. To that end, we fabricated a sample which had an Al_2O_3 pattern consisting of a single 2 μm wide channel but this time at an angle of 13° compared to the direction of current flow ($\hat{y}$). A section of direct contact was fabricated between the Nb and Al layers, which had an area 10 times larger than that of the channel (see Figure 4a). This creates a homogeneous current density in the Nb layer near the channel in the y-direction, so that the contribution from the channel does not affect it significantly and mostly serves to modulate the QP distribution. Figure 4b shows $V(I)$ characteristics for the various leads in the vicinity of the channel. As expected, only a single jump is observed in the voltage when measuring with leads that are positioned across the channel. However, even for substantially higher currents the voltage between leads that do not cross the channel is virtually zero. This is despite the vertical separation (in the y-axis) between the voltage leads, for which vortex flow in the x-direction would result in observation of voltage. This result unequivocally shows that here, vortex flow is confined to the fabricated channel and little or no leakage of vortices is observed outside of it despite the force that is exerted by the current in this direction. This provides evidence that current injection does not merely assist vortex flow but rather it creates a potential landscape for vortices that is able to exert a force that is not in the trivial direction dictated by the current flow. A secondary consequence of the QP injection is that as vortices start flowing in the channel, they may accumulate on its edges due to the relatively high pinning force they encounter there because of the low outer QP occupancy. These pinned vortices may exert a force on the ones flowing in the channel, thus guiding them along its direction.

Whatever the exact guiding mechanism, because the vortices flow in the direction of the channel, the sum of the perpendicular forces must vanish. This holds even for the largest currents we could apply because no vortex flow was ever detected outside the defined channel. The lower bound for the maximum force that can act on vortices to confine their flow to the channel is equivalent to that applied by a current equal to $J_y\sin(\theta) = 1.4 \times 10^5$ A/cm^2, where J_y is the maximum applied current density in the y-direction and θ is the angle of the channel with respect to the x-axis, 13°. This current is only 1 order of magnitude smaller than the typical critical current density in Nb films,[55] indicating that the pinning potential created by inhomogeneous QP distribution is a strong effect.

To conclude, we have found voltage jumps in the $V(I)$ curves of Nb superconducting thin films when current is injected into the films from a normal metal through nanopatterned insulating layers. These jumps are a hallmark of channel-like flow of vortices, and they do not occur in the absence of a pattern. We attribute our findings to inhomogeneous QP distributions that form due to the patterned current injection. These create potential landscapes that induce vortex channeling, which is most efficient for patterns comprising continuous straight lines perpendicular to the current flow. The inhomogeneous QP injection is shown to be able to guide vortices in a direction that deviates from that of the force exerted by the current flow. This paves the way toward using localized current injection to control the vortex potential and their motion in a dynamic way and at the nanoscale. With more elaborate lead configurations for current injection in which the vortex potential created by two adjacent leads overlaps, one might be able to move vortices between adjacent sites by gradually increasing the injected current from one lead while decreasing the other. This may lead to applications in the field of fluxon-based computation, quantum computation using vortex braiding, and for designing nanometric scale magnetic field patterns. Having the ability to tune the intensity and spatial configuration of the vortex potential should also prove valuable for the basic study of vortex matter.

■ ASSOCIATED CONTENT

Supporting Information

The Supporting Information is available free of charge on the ACS Publications website at DOI: 10.1021/acs.nanolett.7b00179.

Sample preparation details, investigation of static pinning potential contribution to channeling effect, channeling multistability (PDF)

■ AUTHOR INFORMATION

ORCID

Yoav Kalcheim: 0000-0002-1489-0505

Present Address

§(Y.K.) Department of Physics and Center for Advanced Nanoscience, University of California, San Diego, La Jolla, California 92093, United States.

Notes

The authors declare no competing financial interest.

■ ACKNOWLEDGMENTS

The research was supported in parts by the Leverhulme Trust, Grant IN-2013-033 and by the ERC Grant 335933. O.M. thanks support from the Harry de Jur Chair in Applied Science.

■ REFERENCES

(1) Campbell, A. M.; Evetts, J. E. *Adv. Phys.* **1972**, *21* (90), 199−428.
(2) Blatter, G.; Feigel'Man, M. V.; Geshkenbein, V. B.; Larkin, A. I.; Vinokur, V. M. *Rev. Mod. Phys.* **1994**, *66* (4), 1125−1388.
(3) Fisher, D. S.; Fisher, M. P. A.; Huse, D. A. *Phys. Rev. B: Condens. Matter Mater. Phys.* **1991**, *43* (1), 130−159.
(4) Chen, B.; Halperin, W. P.; Guptasarma, P.; Hinks, D. G.; Mitrovic, V. F.; Reyes, A. P.; Kuhns, P. L. *Nat. Phys.* **2007**, *3* (4), 239.
(5) Vinokur, V. M.; Feigel'man, M. V.; Geshkenbein, V. B.; Larkin, A. I. *Phys. Rev. Lett.* **1990**, *65* (2), 259−262.
(6) Zeldov, E.; Majer, D.; Konczykowski, M.; Geshkenbein, V. B.; Vinokur, V. M.; Shtrikman, H. *Nature* **1995**, *375* (6530), 373−376.
(7) Bouquet, F.; Marcenat, C.; Steep, E.; Calemczuk, R.; Kwok, W. K.; Welp, U.; Crabtree, G. W.; Fisher, R. A.; Phillips, N. E.; Schilling, A. *Nature* **2001**, *411* (6836), 448−451.
(8) Harada, K.; Kamimura, O.; Kasai, H.; Matsuda, T.; Tonomura, A.; Moshchalkov, V. V. *Science (Washington, DC, U. S.)* **1996**, *274* (5290), 1167−1170.
(9) Martín, J.; Vélez, M.; Nogués, J.; Schuller, I. *Phys. Rev. Lett.* **1997**, *79* (10), 1929−1932.
(10) Rizzo, N. D.; Wang, J. Q.; Prober, D. E.; Motowidlo, L. R.; Zeitlin, B. A. *Appl. Phys. Lett.* **1996**, *69* (15), 2285−2287.

DOI: 10.1021/acs.nanolett.7b00179
Nano Lett. 2017, 17, 2934−2939

(11) Daldini, O.; Martinoli, P.; Olsen, J. L.; Berner, G. *Phys. Rev. Lett.* **1974**, *32* (5), 218−221.
(12) Baert, M.; Metlushko, V. V.; Jonckheere, R.; Moshchalkov, V. V.; Bruynseraede, Y. *Phys. Rev. Lett.* **1995**, *74* (16), 3269−3272.
(13) Van Bael, M. J.; Van Look, L.; Temst, K.; Lange, M.; Bekaert, J.; May, U.; Güntherodt, G.; Moshchalkov, V. V.; Bruynseraede, Y. *Phys. C* **2000**, *332* (1), 12−19.
(14) Raedts, S.; Silhanek, A. V; Van Bael, M. J.; Moshchalkov, V. V. *Phys. Rev. B: Condens. Matter Mater. Phys.* **2004**, *70*, 024509.
(15) Tarantini, C.; Lee, S.; Kametani, F.; Jiang, J.; Weiss, J. D.; Jaroszynski, J.; Folkman, C. M.; Hellstrom, E. E.; Eom, C. B.; Larbalestier, D. C. *Phys. Rev. B: Condens. Matter Mater. Phys.* **2012**, *86* (21), 1−7.
(16) Civale, L.; Marwick, A. D.; Worthington, T. K.; Kirk, M. A.; Thompson, J. R.; Krusin-Elbaum, L.; Sun, Y.; Clem, J. R.; Holtzberg, F. *Phys. Rev. Lett.* **1991**, *67* (5), 648−651.
(17) Navarro, E.; Monton, C.; Pereiro, J.; Basaran, A. C.; Schuller, I. K. *Phys. Rev. B: Condens. Matter Mater. Phys.* **2015**, *92* (14), 144512.
(18) Córdoba, R.; Baturina, T. I.; Sesé, J.; Mironov, a Y.; De Teresa, J. M.; Ibarra, M. R.; Nasimov, D. a; Gutakovskii, a K.; Latyshev, a V; Guillamón, I.; Suderow, H.; Vieira, S.; Baklanov, M. R.; Palacios, J. J.; Vinokur, V. M. *Nat. Commun.* **2013**, *4*, 1437.
(19) Trastoy, J.; Ulysse, C.; Bernard, R.; Malnou, M.; Bergeal, N.; Lesueur, J.; Briatico, J.; Villegas, J. E. *Phys. Rev. Appl.* **2015**, *4* (5), 54003.
(20) Fang, L.; Jia, Y.; Schlueter, J. A.; Kayani, A.; Xiao, Z. L.; Claus, H.; Welp, U.; Koshelev, A. E.; Crabtree, G. W.; Kwok, W.-K. *Phys. Rev. B: Condens. Matter Mater. Phys.* **2011**, *84* (14), 140504.
(21) Savel'ev, S.; Nori, F. *Nat. Mater.* **2002**, *1* (3), 179−184.
(22) Velez, M.; Martin, J. I.; Villegas, J. E.; Hoffmann, A.; Gonzalez, E. M.; Vicent, J. L.; Schuller, I. K. *J. Magn. Magn. Mater.* **2008**, *320* (21), 2547−2562.
(23) Villegas, J. E.; Gonzalez, E. M.; Gonzalez, M. P.; Anguita, J. V.; Vicent, J. L. *Phys. Rev. B: Condens. Matter Mater. Phys.* **2005**, *71* (2), 24519.
(24) del Valle, J.; Gomez, A.; Gonzalez, E. M.; Osorio, M. R.; Granados, D.; Vicent, J. L. *Sci. Rep.* **2015**, *5*, 15210.
(25) Olson Reichhardt, C. J.; Wang, Y. L.; Xiao, Z. L.; Kwok, W. K.; Ray, D.; Reichhardt, C.; Jankó, B. *Phys. C* **2017**, *533*, 148−153.
(26) Zhu, B. Y.; Marchesoni, F.; Moshchalkov, V. V.; Nori, F. *Phys. Rev. B: Condens. Matter Mater. Phys.* **2003**, *68* (1), 14514.
(27) Zhu, B. Y.; Marchesoni, F.; Nori, F. *Phys. Rev. Lett.* **2004**, *92* (18), 180602.
(28) Rezaev, R. O.; Levchenko, E. A.; Fomin, V. M. *Supercond. Sci. Technol.* **2016**, *29* (4), 045014.
(29) Fomin, V. M.; Rezaev, R. O.; Schmidt, O. G. *Nano Lett.* **2012**, *12* (3), 1282−1287.
(30) Kremen, A.; Wissberg, S.; Haham, N.; Persky, E.; Frenkel, Y.; Kalisky, B. *Nano Lett.* **2016**, *16* (3), 1626−1630.
(31) Veshchunov, I. S.; Magrini, W.; Mironov, S. V.; Godin, A. G.; Trebbia, J.-B.; Buzdin, A. I.; Tamarat, P.; Lounis, B. *Nat. Commun.* **2016**, *7*, 12801.
(32) Ge, J.-Y.; Gladilin, V. N.; Tempere, J.; Xue, C.; Devreese, J. T.; Van de Vondel, J.; Zhou, Y.; Moshchalkov, V. V. *Nat. Commun.* **2016**, *7*, 13880.
(33) Roditchev, D.; Brun, C.; Serrier-Garcia, L.; Cuevas, J. C.; Bessa, V. H. L.; Milosevic, M. V.; Debontridder, F.; Stolyarov, V.; Cren, T. *Nat. Phys.* **2015**, *11* (4), 332−337.
(34) Gray, K. E. *Nonequilibrium Superconductivity, Phonons and Kapitza Boundaries*; Plenum: New York, 1981.
(35) Tinkham, M. *Introduction to Superconductivity*; McGraw-Hill, Inc., 1996.
(36) Blamire, M. G.; Kirk, E. C. G.; Evetts, J. E.; Klapwijk, T. M. *Phys. Rev. Lett.* **1991**, *66* (2), 220−223.
(37) Andreev, A. F. *Sov. Phys. JETP* **1965**.
(38) Pippard, A. B.; Shepherd, J. G.; Tindall, D. A. *Proc. R. Soc. London, Ser. A* **1971**, *324*, 17−35.
(39) Yu, M. L.; Mercereau, J. E. *Phys. Rev. B* **1975**, *12* (11), 4909.
(40) Scalapino, D. J.; Huberman, B. A. *Phys. Rev. Lett.* **1977**, *39* (21), 1365−1368.
(41) Dynes, R. C.; Narayanamurti, V.; Garno, J. P. *Phys. Rev. Lett.* **1977**, *39* (4), 229−232.
(42) Iguchi, I.; Langenberg, D. N. *Phys. Rev. Lett.* **1980**, *44* (7), 486−489.
(43) Henderson, W.; Andrei, E. Y.; Higgins, M. J.; Bhattacharya, S. *Phys. Rev. Lett.* **1996**, *77* (10), 2077−2080.
(44) Jensen, H. J.; Brass, A.; Berlinsky, A. J. *Phys. Rev. Lett.* **1988**, *60* (16), 1676−1679.
(45) D'Anna, G.; Gammel, P. L.; Safar, H.; Alers, G. B.; Bishop, D. J.; Giapintzakis, J.; Ginsberg, D. M. *Phys. Rev. Lett.* **1995**, *75* (19), 3521−3524.
(46) Gronbech-Jensen, N.; Bishop, A. R.; Domínguez, D. *Phys. Rev. Lett.* **1996**, *76* (16), 2985.
(47) Shi, D. Q.; Xu, X. B.; Zhu, X. B.; Wang, L.; Li, Q.; Dou, S. X. *Phys. C* **2010**, *470*, S836−S837.
(48) Rusanov, A. Y.; Hesselberth, M. B. S.; Aarts, J. *Phys. Rev. B: Condens. Matter Mater. Phys.* **2004**, *70* (2), 24510.
(49) Xu, K.; Cao, P.; Heath, J. R. *Nano Lett.* **2010**, *10* (10), 4206−4210.
(50) Dinner, R. B.; Robinson, A. P.; Wimbush, S. C.; MacManus-Driscoll, J. L.; Blamire, M. G. *Supercond. Sci. Technol.* **2011**, *24* (5), 055017.
(51) Larkin, A. I.; Ovchinnikov, Y. N. In *Nonequilibrium Superconductivity*; Langenberg, D. N., Larkin, A. I., Eds.; North Holland, 1986; pp 493−542.
(52) Vodolazov, D. Y.; Peeters, F. M. *Phys. Rev. B: Condens. Matter Mater. Phys.* **2007**, *76* (1), 14521.
(53) Tidecks, R. *Springer Tracts Mod. Phys.* **1990**, *121*, 269.
(54) Kadin, A. M.; Goldman, A. M. In *Nonequilibrium Superconductivity*; Langenberg, D. N., Larkin, A. I., Eds.; Elsevier Science: Berlin, 1986; p 254.
(55) Huebener, R.; Kampwirth, R.; Martin, R.; Barbee, T.; Zubeck, R. *IEEE Trans. Magn.* **1975**, *11* (2), 344.

DOI: 10.1021/acs.nanolett.7b00179
Nano Lett. 2017, 17, 2934−2939